Impact of Thermal Transfer on Hydration Heat of a Soundless Chemical Demolition Agent

Debra F. Laefer[a], Atteyeh S. Natanzi[b], S.M. Iman Zolanvari[c]

[a]Center for Urban Science and Progress and the Department of Civil and Urban Engineering, Tandon School of Engineering, New York University, 370 Jay St.,12th Fl., Brooklyn, NY 11201, USA; debra.laefer@nyu.edu

[b]Urban Modelling Group, School of Civil Engineering, University College Dublin, Belfield, Dublin 4, Ireland; atteyeh.natanzi@ucdconnect.ie

[c]Urban Modelling Group, School of Civil Engineering, University College Dublin, Belfield, Dublin 4, Ireland; iman.zolanvari@ucdconnect.ie

Corresponding Author: Debra F. Laefer, debra.laefer@nyu.edu

Abstract: This paper explores thermal transfer effects in Soundless Chemical Demolition Agents (SCDA). In a 10˚C water bath, quadrupling the volume of SCDA in a pipe accelerated peak hydration onset and resulted in a 700% increase in expansive pressure and a 20% increase in volumetric expansion. An equivalent sample in a constant temperature chamber showed almost 5°C greater hydration heat than in the water bath, which resulted in a six-fold expansive pressure difference after 4 days of testing and an order of magnitude more pressure in the first 24 hours, thereby demonstrating limitations of previous SCDA experimental work and providing a temperature based reason for discrepancies between large-scale testing and manufacturers' predictions. Since most construction projects have scheduling requirements, understanding how to achieve sufficiently high pressures within a single work shift is important for evaluating the field viability of SCDAs on a particular project.

Keywords: Soundless Chemical Demolition Agent, Expansive Cement, Ambient Temperature, Borehole Diameter, Non-Expansive Demolition Agent, Thermal Transfer, Bristar, Heat of Hydration, Volumetric Expansion, Expansive Pressure.

1 INTRODUCTION

Building standards and environmental policies demand a high level of control when undertaking structural demolition. Consequently, use of heavy demolition equipment and explosives has been restricted in urban areas due to their unwanted side effects of noise, debris, and vibrations. Soundless Chemical Demolition Agents (SCDAs) offer an alternative by means of chemically-based selective material removal. However, to date there has not been a full understanding of the development of the hydration heat and its subsequent expansive pressure gains due to several competing factors including ambient temperature, thermal transfer mechanisms, and SCDA volume. As such, this paper explores SCDA hydration heat and expansive pressure development in various pipe diameters for a commercial product under a temperature common for fieldwork with a control mechanism for thermal transfer.

2 BACKGROUND

SCDAs or Non-Explosive Materials (NEEMs) were first identified in the 1890s by Cadlot and Micheaelis [1] but not commercialized until 1979 in Japan [2]. In 1981, study of SCDAs started in China resulting in a highly efficient soundless cracking agent with expansive pressures of 60-90 MPa only 2 years later [3]. By 1985, a fast acting commercial SCDA was produced in Japan that developed expansive pressure in only 3 hours and was sufficient for cracking small concrete samples (600*600*600 mm^3) [2]. Today's market includes many commercial SCDA products that promise initial cracking within a few hours including Dexpan (http://www.dexpan.com/), Bristar (http://www.taiheiyo-m.co.jp/), Betonamit (http://www.betonamit.net/), Cevamit (http://cevamit.cz/), and S-Mite (http://www.soc.co.jp/). The environmental conditions under which such cracking can be expected, however, are not fully

described by the manufacturers and are often difficult to replicate in lab conditions, as previously demonstrated by Laefer et al. [4] and Huynh et al. [5] where cracking times were significantly slower than advertised. In those tests, the large concrete blocks (0.67 m^3 – 1.0 m^3) surrounding the embedded SCDA were likely to have served as heat sinks and to have interfered with the rate and possibly the maximum level of thermal development within the SCDA.

Generically, SCDAs can be described as powdery materials, similar in texture and appearance to Portland cement [6]. These are mixed with water to be introduced as a slurry into a series of predrilled holes. SCDAs mainly consist of calcium oxide (CaO). Other components may include ferrous oxide (Fe_2O_3), magnesium oxide (MgO), aluminium oxide (Al_2O_3), silicon (SiO_2), sulfur trioxide (SO_3) and calcium fluoride (CaF_2) and are designed to delay, accelerate, or just generally control the hydration rate of the slurry [7], as described in further detail below. The water initiates the hydration process. The reaction of the CaO generates heat and calcium hydroxide ($Ca(OH)_2$), as described by Goto et al. [8]:

$$CaO + H_2O \rightarrow Ca(OH)_2 + 15.2 \uparrow (kCal/mol) \quad (1)$$

If not properly controlled, this SCDA hydration heat may reach temperatures in excess of 150°C, causing the mix water to boil and resulting in the SCDA mixture being expelled from the hole into which it was inserted [9]. Hydration of CaO and formation of $Ca(OH)_2$ are considered the main reactions in this process that generate notable expansive stresses. The formation of ettringite is a secondary contribution in expansive pressure development. Other cementing materials such as calcuim silicate (in the form of belite or alite) and calcium aluminates (which is generated by calcium oxide and aluminium oxide – the main SCDA components) are present in the SCDA mixture. For example, calcium silicate (in the form of belite) was reported by Soeda

72 and Harada [14], and the SCDA manufacturer's product literature used in herein (Bristar 150),
73 reports the presence of calcium silicate in the forms of both alite and belite (10-20% by weight)
74 [15]. When the SCDA-generated stresses exceed the tensile strength of the surrounding
75 materials, cracks will form and then propagate over time [10].

76 As will be discussed below, SCDAs can be highly influenced by temperature-related
77 factors. Manufacturers recommend SCDA selection based on the lowest ambient temperature
78 likely to be encountered, and specific SCDAs are designed for particular ambient temperature
79 ranges as low as -8°C and as high as 50°C [11]. A higher ambient temperature will result in
80 earlier and greater expansive pressures. This was demonstrated by Laefer et al. [4] in tests on
81 0.67 m^3 concrete blocks with small aggregate. That study also demonstrated that the time to first
82 crack (TFC) was reduced by 13 hours and the minimum demolition time (MDT) [time when the
83 sample can be mechanically dismantled] was decreased by 4 hours, when the ambient
84 temperature was increased by 14°C (from 24°C to 38°C). Unfortunately, direct pressure gains
85 could not be measured in that experimental set up. Similar work by Huynh et al. [5] in 1 m^3
86 unreinforced concrete blocks showed that increasing ambient temperature by almost 3°C
87 decreased the TFC by almost 4 hours and accelerated MDT by almost 5 hours. Notably, in those
88 two studies, the surrounding concrete blocks served as large thermal sinks, as opposed to most
89 SCDA research, which has been conducted in steel pipes, to facilitate direct pressure
90 measurement.

91 For example, in the work by Hinze and Brown [7] in 100 mm high, 43 mm diameter,
92 thick walled, steel pipes there was a doubling of expansive pressure when the ambient
93 temperature was increased from 20°C to 30°C. Similarly, in the work by Natanzi et al. [9] on the
94 impact of cold and moderate ambient temperatures, SCDA expansive pressure in 170 mm high,

95 36 mm diameter steel pipes increased by 350% when the temperature was raised from 2°C to
96 19°C. Onoda [12] reported less dramatic gains in thin-walled, steel cylinders of indeterminate
97 size with a 30% pressure rise in the first 24 hours and only a 10% difference after 48 hours when
98 the ambient temperature was increased from 15°C to 25°C.

99 Ambient temperature also affects the rate and magnitude of expansion due to the impact
100 on ettringite formation during hydration [13]. Additionally, higher ambient temperatures result in
101 faster exothermic hydration reactions, thus increasing $Ca(OH)_2$ generation [14]. Experimental
102 work by Soeda et al. [16] showed a direct relationship between greater hydration level formation
103 and increased expansive pressure development. Experimental results by Natanzi et al. [9] also
104 demonstrated faster exothermic reactions at higher ambient temperatures, which hastened peak
105 hydration heat and, in turn, generated greater and earlier expansive pressure development.

106 While this linkage has been definitively established, the issue of borehole size and its
107 effect, if any, on expansive pressure development has been less clear. Hinze and Brown [7]
108 investigated borehole diameter variation with a Chinese SCDA in 100 mm high steel cylinders of
109 4 different diameters (25mm, 38mm, 43mm and 50mm) at an ambient temperature 33°C and a
110 water/SCDA ratio of 32%. After 8 hours, the 25 mm diameter hole reached an expansive
111 pressure of only 2 MPa, while the 38 mm and 43 mm diameter holes generated pressures of
112 3 MPa and 4.5 MPa, respectively. Furthermore, the 50 mm diameter specimen reached 7 MPa.
113 However, the authors concluded that specimen diameter was not a significant factor based on the
114 fact that all of the specimens had nearly identical expansive pressures after 24 hours.

115 In laboratory tests by Dowding and Labuz [17], the product Bristar 100 was poured into
116 100 mm high, thick-walled, steel cylinders of different diameters (102 mm and 172 mm). After
117 48 hours, the expansive pressures were highly similar to each other. These results seemed to

contravene their field tests on dolomite blocks (unconfined compressive strength of 165 MPa), where wider boreholes (38.0 mm vs. 12.7 mm) developed faster expansive pressures, as would be expected due to the larger amount of material available for hydration. After 18 hours in the field, the 38 mm borehole block cracked and reached approximately 40% of the size of the borehole after 90 hours. In contrast, the 12.7 mm borehole did not crack until 42 hours and only managed a crack width of 3% of the borehole, implying that larger boreholes exhibit both a more rapid development of expansive pressure and ultimately more pressure overall, although this was not measured directly.

Schram and Hinze [18] stated that for effective rock fracturing both hole diameter and configuration were critical. For large granite rocks and boulders, they recommended a minimum effective borehole diameter of 38 mm. They also stated that a borehole diameter range of 44-50 mm provided the maximum amount of rock fracturing per pound of SCDA. In research by Gambatese [6], Betonamit Type S was poured into small-scale (152.4 mm*152.4 mm*76.2 mm) reinforced concrete blocks (20.7 MPa concrete mix design) with boreholes of different diameters (3.18 mm, 4.76 mm, and 6.35 mm) but of the same lengths. Those tests showed that small borehole diameters were still sufficient to generate enough expansive pressure for cracking relatively strong concrete, although direct pressure measurements were not made.

Theoretically, increasing the borehole diameter should result in more CaO, which in turn should lead to a more acute exothermic reaction and, subsequently, more $Ca(OH)_2$ generation. The greater heat of hydration, which was likely the result of a more complete chemical reaction, leads to higher expansive pressure development and more $Ca(OH)_2$ generation. To date this has only been discussed with respect to two-dimensional (2D) development, but in fact the wide range of thermal development showed by Natanzi et al. [9] across a 36 mm diameter, 170 mm

high specimen clearly demonstrates the three-dimensional (3D) and likely volumetric dependencies of the problem. Furthermore, thermal transfer is an interference mechanism in the hydration heat development and, in turn, in the pressure development.

The experiments presented herein were designed specifically to gain further insight into these issues. Importantly, many of the studies conducted to date have focused only on the final maximum achievable stress, irrespective of the required duration. Since most construction projects do not have this temporal luxury, understanding how to achieve high (but controllable) pressures within a single work shift or cycle (8-12 hours) is quite critical. Presently, there has been no systematic study of SCDA heat development in different hole diameters or considering thermal transfer effects. Understanding these factors is important to designing SCDA fieldwork, as hydration heat development is indicative of expansive pressure development and can result in additional thermal stresses [19].

3 PROJECT SCOPE AND METHODOLOGY

3.1 Scope

This study investigates the impact of borehole diameter and volume, as well as the thermal transfer with respect to the relationship between the heat of hydration, expansive pressure, thermal transfer, and volume growth in a commercial SCDA tested at 10°C. This was based on the work by Natanzi et al. [9] that demonstrated experimentally that an ambient temperature of 10°C marked a critical point for Bristar, as pressure and temperature gains were non-linear below this temperature).

3.2 Testing methods

This paper investigates these issues with the commercial SCDA Bristar 150. According to the manufacturer, Bristar 150 is designed for temperatures up to 20°C with no lower bound temperature specified. The Bristar was mixed according to the manufacturer's recommendations (tap water at 15°C; 30% by weight). The slurry was poured into 50.8 mm, 76.2 mm, and 101.6 mm diameter seamless, stainless steel pipes each of 500 mm in length. To investigate the effect of thermal transfer, the SCDA filled pipes were placed vertically into a water bath with a temperature of 10°C±0.3°C (Figure 1b) controlled continuously through the introduction of hot water or ice into the surrounding water.

The hydration heat produced during the SCDA curing was measured throughout the testing period using thermocouples embedded in the SCDA at five locations: in the water bath, in the air surrounding the test set up, and at the top, middle, and bottom of each pipe. The expansive pressure was measured with three sets of strain gauges affixed to the outside of the pipe (top, middle, and bottom). Tangential strains and temperatures were recorded in intervals of 0.1s and 1s, respectively.

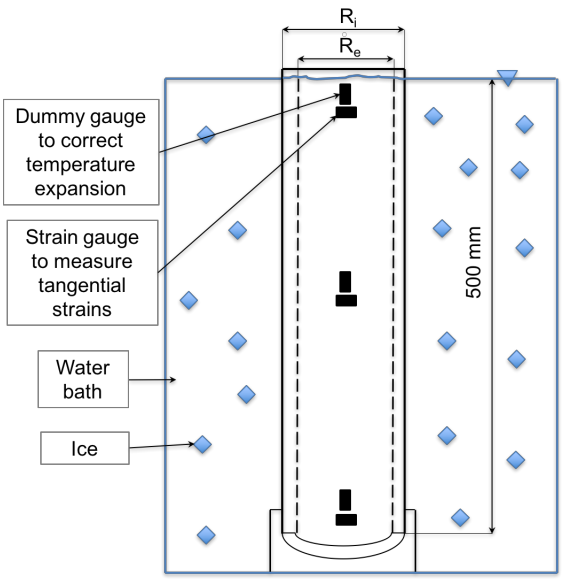

(a) Steel pipe dimensions and strain gauge orientations

(b) Photograph of 76.2 mm sample in the water bath

Figure 1. Testing configuration for large steel pipes in a water bath

3.3 Evaluation Methods

The expansive pressure was calculated using the theory of elasticity. According to Timoshenko and Goodier [20], tangential and radial stresses in a thick-walled cylinder under a uniform internal and external load are a function of pressure:

$$\sigma_r = \frac{R_i^2 P_e - R_e^2 P_e}{(R_e^2 - R_i^2)} - \frac{(P_i - P_e) R_i^2 R_e^2}{(R_e^2 - R_i^2) r^2} \quad (2)$$

$$\sigma_\theta = \frac{R_i^2 P_i - R_e^2 P_e}{(R_e^2 - R_i^2)} + \frac{(P_i - P_e) R_i^2 R_e^2}{(R_e^2 - R_i^2) r^2} \quad (3)$$

σ_r : radial tangential stresses

σ_θ : tangential stresses

P_i : internal pressures

P_e : external pressures

R_i : internal radii

R_e : external radii

r : radial distance to the point of interest

185 The strain gauges were placed on the external boundary where $\sigma_r = 0$. During testing, there was
186 no external pressure on the pipe ($P_e = 0$). Therefore, the tangential stress on the external
187 boundary ($r = R_e$) can be expressed by (4):

$$\sigma_\theta = \frac{2P_i R_i^2}{(R_e^2 - R_i^2)} \tag{4}$$

188 The tangential strain on the external boundary of the cylinder is as per (5):

$$\varepsilon_\theta = \frac{1}{E}(\sigma_\theta - \sigma_r) = \frac{\sigma_\theta}{E} = \frac{2P_i R_i^2}{E(R_e^2 - R_i^2)} \tag{5}$$

189 Expansive pressure is represented by (6):

$$P_i = \frac{\varepsilon_\theta E(R_e^2 - R_i^2)}{2R_i^2} \tag{6}$$

190 The tangential strain ε_θ is the output given by the strain gauges employed in this testing, and the
191 modulus of elasticity of the steel was E=180 GPa.

192

193 The pipe was considered a thick-walled steel cylinder based on Hertzberg's criterion [21]:

$$K = \frac{R_e - R_i}{R_i} > \frac{1}{20} \tag{7}$$

where R_i is the internal and R_e is the external radius. The external and internal diameters were chosen to satisfy the thick-walled criterion (Table 1).

Table 1. External and Internal diameter for the thick-walled criterion

Pipe Diameter (mm)	R_e (mm)	R_i (mm)	K
50.8	26.14	21.74	0.2024
76.2	44.56	38.36	0.1616
101.6	56.91	50.98	0.1163

The selected 500 mm long pipe (Figure 1) was deemed as adequate to crack a rock or concrete specimen to a depth of around 700 mm according to a 70% depth rule developed by Huynh and Laefer [22]. Next, the cylinder was closed at one end with a welded cap to simulate field conditions. Lastly, a simple clamp, also submerged in the water, was attached to a heavy plate to hold the cylinder upright during testing.

Half a dozen sets of 5 mm long strain gauges with an original resistance of 120 ohms were affixed to opposite sides of the steel cylinder in the top, middle, and bottom parts to measure tangential strain. The strain gauges were placed in different places to investigate the pressure difference along the pipe and included tangential strain gauges and a dummy gauge to correct for thermal expansion using a Wheatstone bridge circuit arrangement (Figure 1a). A further dummy gage was not necessary, as the strain gauges on each pipe were calibrated through controlled loading testing in the lab.

The heat of hydration was monitored during testing with a thermocouple located within the SCDA in the top, middle, and bottom of the steel pipe. The thermocouples were placed using pre-measured lengths of wire that were embedded during the introduction of the SCDA slurry. For each test, the SCDA's expansive pressure and hydration heat development were investigated

for four days – selected as the likely longest period a contractor could effectively wait for material removal on an active construction site. At the end of testing, vertical expansion of the material at the top of the pipe was measured with Vernier calipers; radial pipe expansion was previously established experimentally as negligible [9].

4 EXPERIMENTAL RESULTS

The three areas for which data were collected related to (1) heat of hydration, (2) expansive pressure, and (3) volumetric expansion.

4.1 Heat of hydration

Figures 2-4 show the ambient air temperature, the surrounding water temperature, and the SCDA temperature caused by the heat of hydration at the top, middle, and bottom of the 50.8 mm, 76.2 mm, and 101.6 mm pipes, respectively. The specimens tended to differ in three aspects: (1) the peak temperatures achieved; (2) the characteristics of the peak temperature development duration; and (3) the timing of that development. Within each sample there were also temperature distributions that needed exploration.

Notably, temperatures recorded at the top of the pipes appear to have been influenced by the ambient temperature. Thus, discussion of the results will focus on the mid-pipe behaviour, as the water bath was used intentionally to replicate the heat sink of surrounding rock or concrete typically found in SCDA field usage (e.g. beneath Carnegie Hall in New York City [23]). These mid-height results showed that, in nearly identical surrounding water temperatures, the peak SCDA hydration heat was higher in larger diameter pipes. The differences were clearly visible (Figures 2-4).

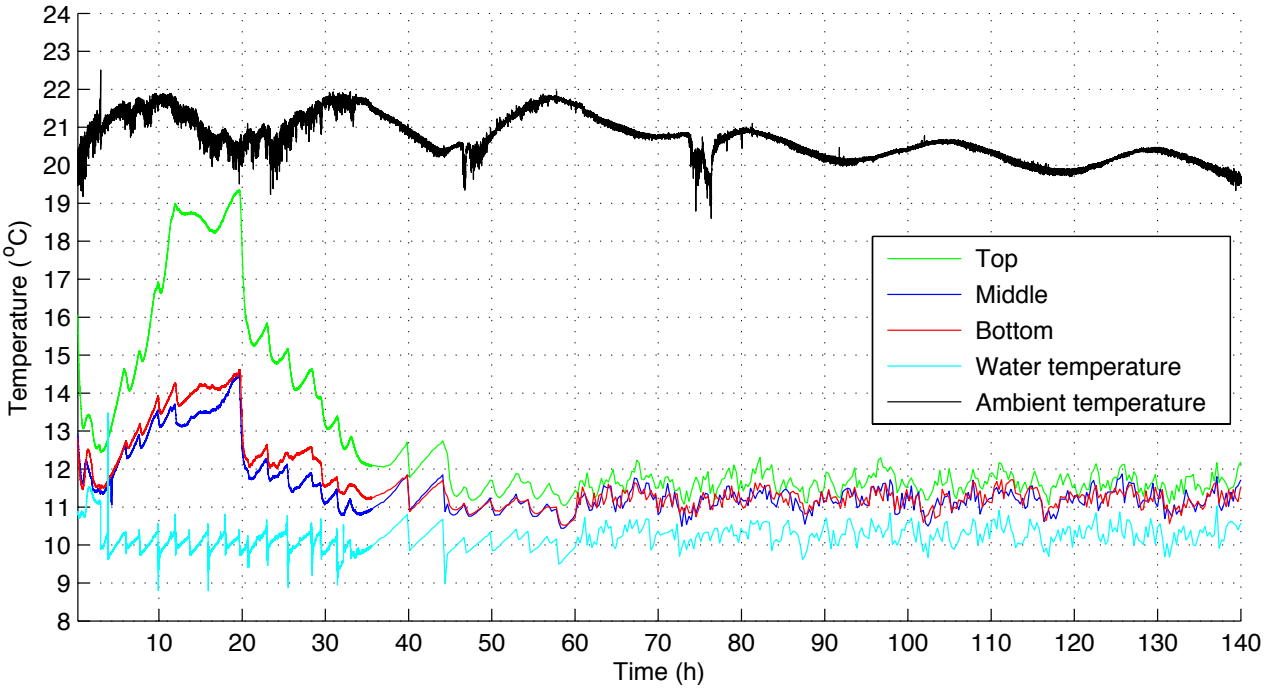

237

238 **Figure 2.** Heat of hydration generation and progress in the 101.6 mm pipe

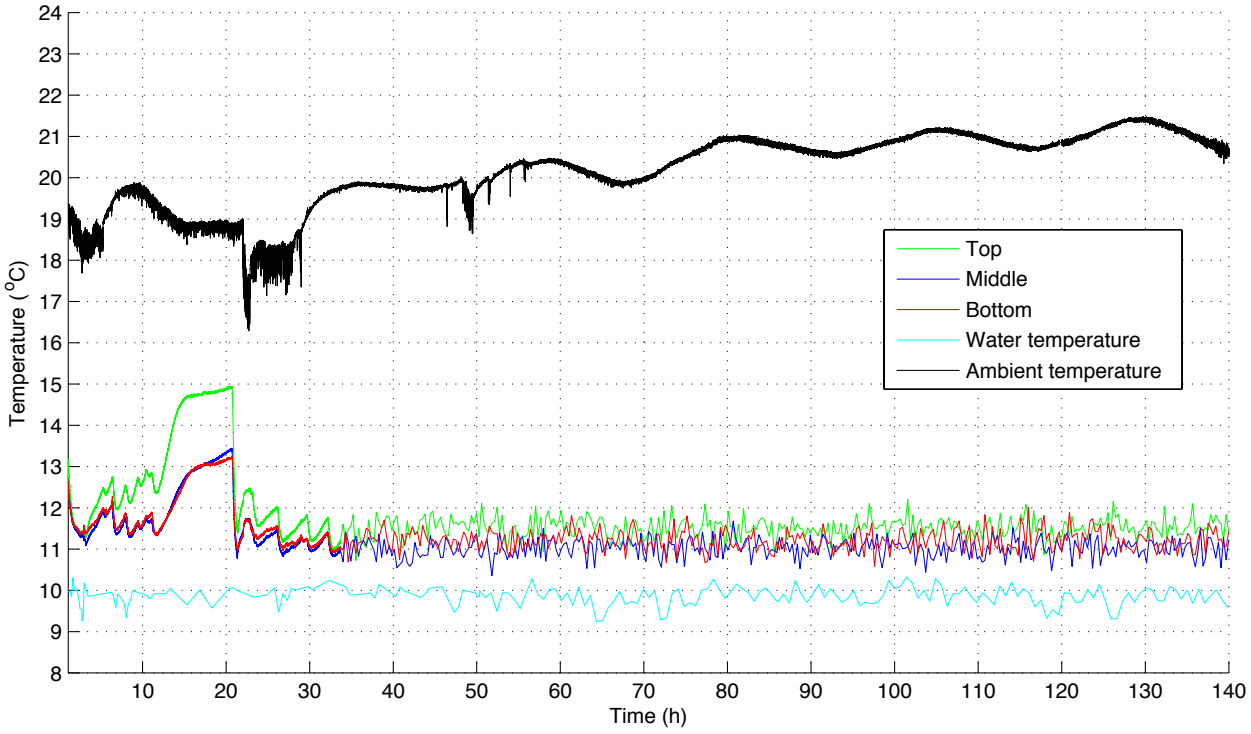

239

240 **Figure 3.** Heat of hydration generation and progress in the 76.2 mm pipe

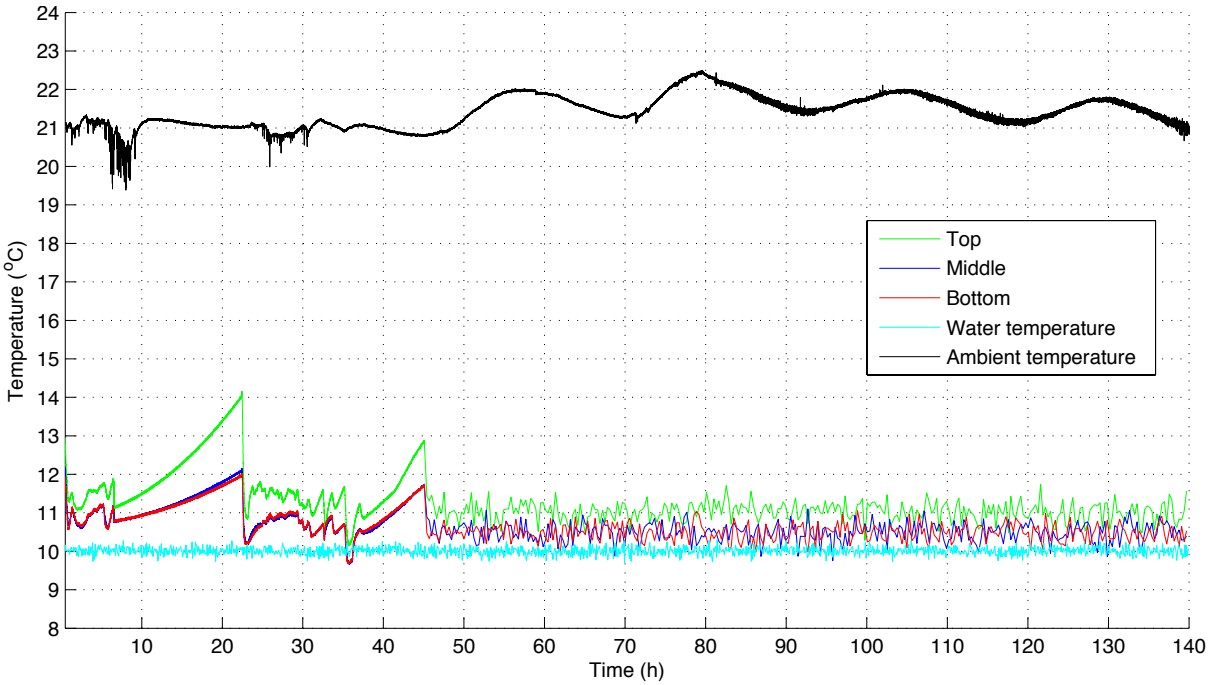

241

242 **Figure 4.** Heat of hydration generation and progress in the 50.8 mm pipe

243 The largest diameter pipe had a peak hydration heat temperature almost 50% greater than
244 the surrounding 10°C water versus only about 22% greater for the smallest pipe (14.62°C vs.
245 12.24°C). In addition, pipe diameter also influenced the shape of the temperature development.
246 A larger pipe diameter generated a more distributed temperature development (likely due to the
247 larger amount of material undergoing hydration). As the pipe diameter narrowed so did the
248 temperature peak, which was quite acute in the smallest diameter pipe (Figure 4). Furthermore, a
249 phenomenon that occurred in only that pipe was a pair of hydration peaks (the first around 22
250 hours and the second at about 48 hours). The cause for this was not immediately evident.

251 Another impact of pipe size was the rate at which the hydration heat developed. Figure 5
252 shows the temperature changes in the first 24 hours. After 20 hours, the peak hydration heat
253 formed in the largest pipe and the medium sized pipe had reached 99.3% of its peak temperature,
254 but the narrowest pipe was only at 96% of its peak temperature. Critically when considered

255 within an 8-12 hour work shift time frame, the largest diameter pipe at 10 hours generated a
256 higher temperature at mid-pipe than the middle-sized pipe did at 20 hours and exceeded the
257 maximum temperature ultimately achieved by the narrowest pipe during the 4 day testing period
258 (Figure 5).

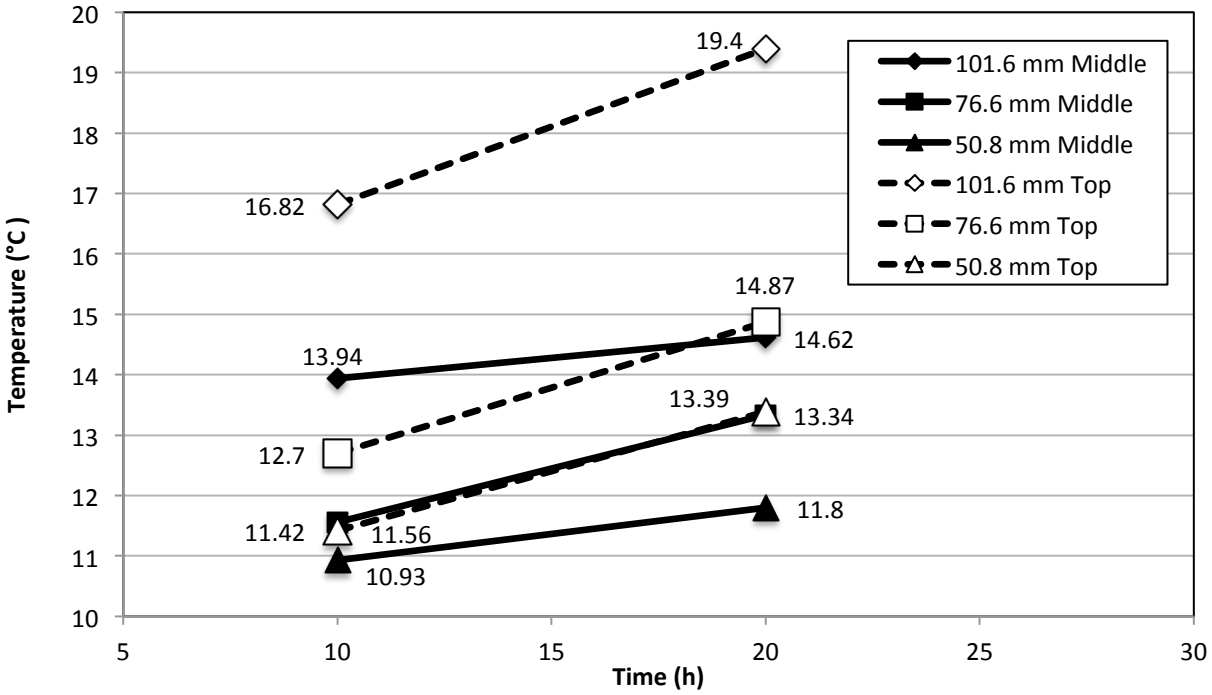

259

260 **Figure 5.** Mid-height SCDA temperature in pipes of varying diameter after 10 and 20 hours

261 Similarly, time to peak SCDA temperature (peak hydration heat) was faster in the larger
262 diameter pipes. Specifically, doubling the pipe diameter (i.e. quadrupling the volume)
263 accelerated the time to the onset of peak hydration heat generation by almost 177% (Figure 6). In
264 the 101.6 mm diameter pipe, this occurred after about 3.29 hours, but required a further 0.22
265 hours (3.51 hours total) for the 76.2 mm pipe and a nearly doubling of time to 5.8 hours for the
266 50.8 mm diameter specimen (Figure 6). The relative temporal closeness of this event in the two
267 larger specimens, in comparison to the smallest would imply that a certain minimum amount of

material undergoing hydration is needed to generate a peak temperature. So, while Figure 6 shows a non-linear relationship between pipe diameter and hydration acceleration, there is a nearly linear relationship between pipe diameter and peak temperature at the pipes' mid-heights, thereby implying that ambient temperature may have had an influence at the top of the pipes.

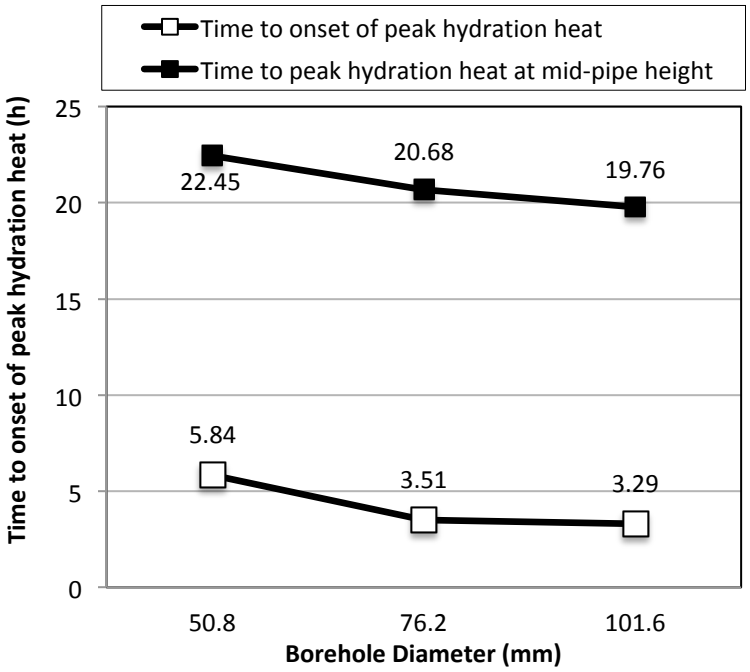

Figure 6. Time to peak hydration heat as a function of borehole diameter

Table 2 shows the peak temperature within the pipes' three measured locations. Also included in this table is a comparative sample that was placed in a temperature-controlled air chamber, which was insufficiently large to accommodate the other two samples. As previously explained in the methodology, the aim of the water bath was to better replicate field conditions. The water-bath samples showed significant temperature differences along the pipes' lengths, with the tops being clearly hotter (Table 2); influenced by the air. The results were very consistent. Temperatures increased with pipe diameter, and the SCDA was hotter the closer it was to the top (Table 2). As with the other factors reported herein, the impact on the larger

specimens was more profound. There was a more than 4.5°C difference between the top thermocouple and the other thermocouples within the 101.8 mm pipe, but only a 1.5-2.0°C difference in the 50.8 mm and 76.2 mm pipes.

Table 2. Temperature of peak of hydration heat in the pipes along with ambient temperature at that time

Pipe diameter (mm)	Test	Ambient	Top	Middle	Bottom
101.6	Water	20.96°C	19.30°C	14.62°C	14.49°C
76.2	Water	18.87°C	14.82°C	13.43°C	13.22°C
50.8	Water	21.0°C	14.11°C	12.24°C	12.10°C
50.8	Chamber	10.0°C	14.34°C	16.20°C	17.79°C

In contrast, the air chamber test in a 10°C arrangement with no external temperature gradient produced a sample that was much hotter at the bottom (more than 5.5°C hotter than the equal diameter pipe in the water test); as shown in detail in Figure 7. As will be further illustrated in the next section and as previously demonstrated by Natanzi et al. [9], accurate estimation of peak temperature was critical for expansive pressure estimation. Also, the time to the onset of peak of hydration in the chamber was faster than in the water bath (3.6 hours vs. 5.84 hours).

Behaviour in the critical, initial 24 hours also differed notably between the chamber and water bath samples. For the chamber sample, peak hydration heat was almost finished after 20 hours, while the water bath sample was only at 96.4% of its peak and 4°C degrees less than the

chamber specimen. Importantly, after 10 hours, the heat of hydration of the chamber was 15.89°C at the middle and 17.75°C at bottom of pipe – very close to its peak of 17.79°C.

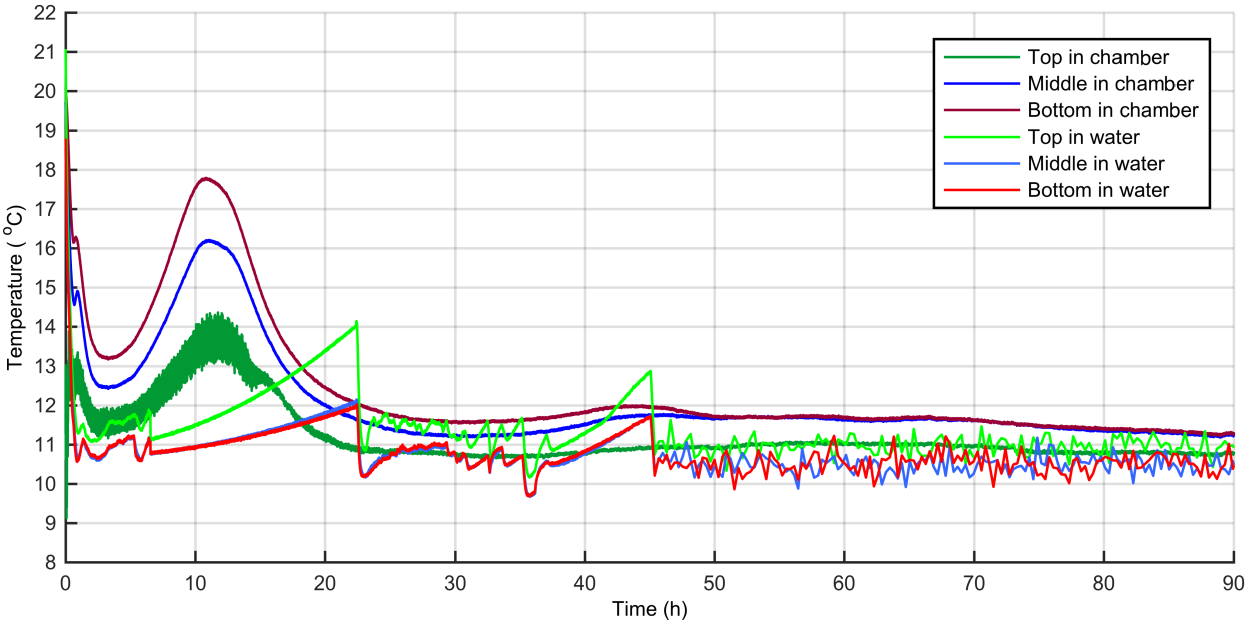

Figure 7. Heat of hydration generation and progress in 50.8 mm pipe in temperature -controlled chamber environment at 10 °C versus that in the water bath

There was a difference in peak hydration at the top, middle, and bottom of the pipe in the controlled chamber environment. This difference in the peak hydration temperature at the top of the pipe is attributable to the direct contact of the SCDA with the air inside the chamber, which reduced the heat of hydration and $Ca(OH)_2$ generation by carbonation of CaO. Unlike the air above the water bath, in the chamber, the surrounding air is cooler than in the specimen. Also, as shown in an affiliated study, hydration seemed to be more complete at the bottom of the pipe and produced more heat of hydration and expansive pressure (Natanzi [24]). The difference between peak hydration heat at middle and bottom of the pipe was only around 1.5°C

4.2 Expansive Pressure

In the water bath experiments, expansive pressure development was higher at the middle of the pipe (Figs. 8-11). The pipe bottoms had slightly lower expansive pressure and hydration heat levels than those recorded at mid-height. At the tops of the pipes, expansive pressure failed to develop because of the lack of vertical constraint. The material expanded upward out of the pipe, and only minimal tangential strain (less than 1 MPa) was measured. In preparatory work done by the authors, SCDA cured in a loose plastic bag showed little change, while the same material at the same temperature in a plastic bottle and glass beaker developed sufficient pressure to destroy the two surrounding vessels.

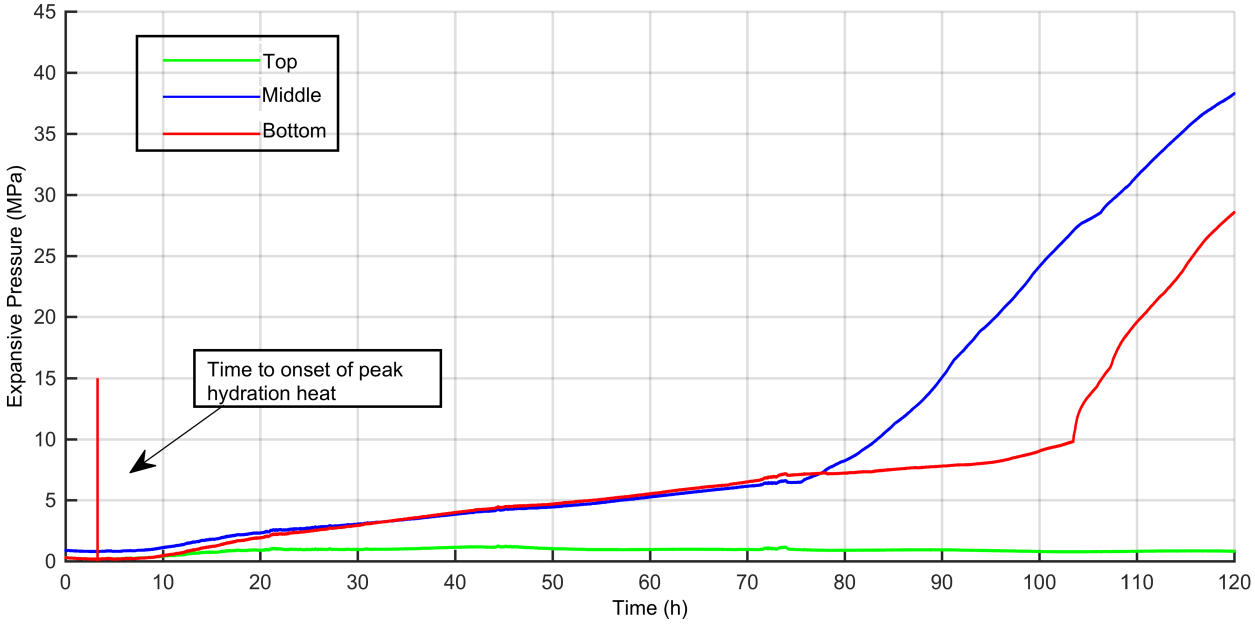

Figure 8. Expansive pressure development over 120 hours in the 101.6 mm pipe

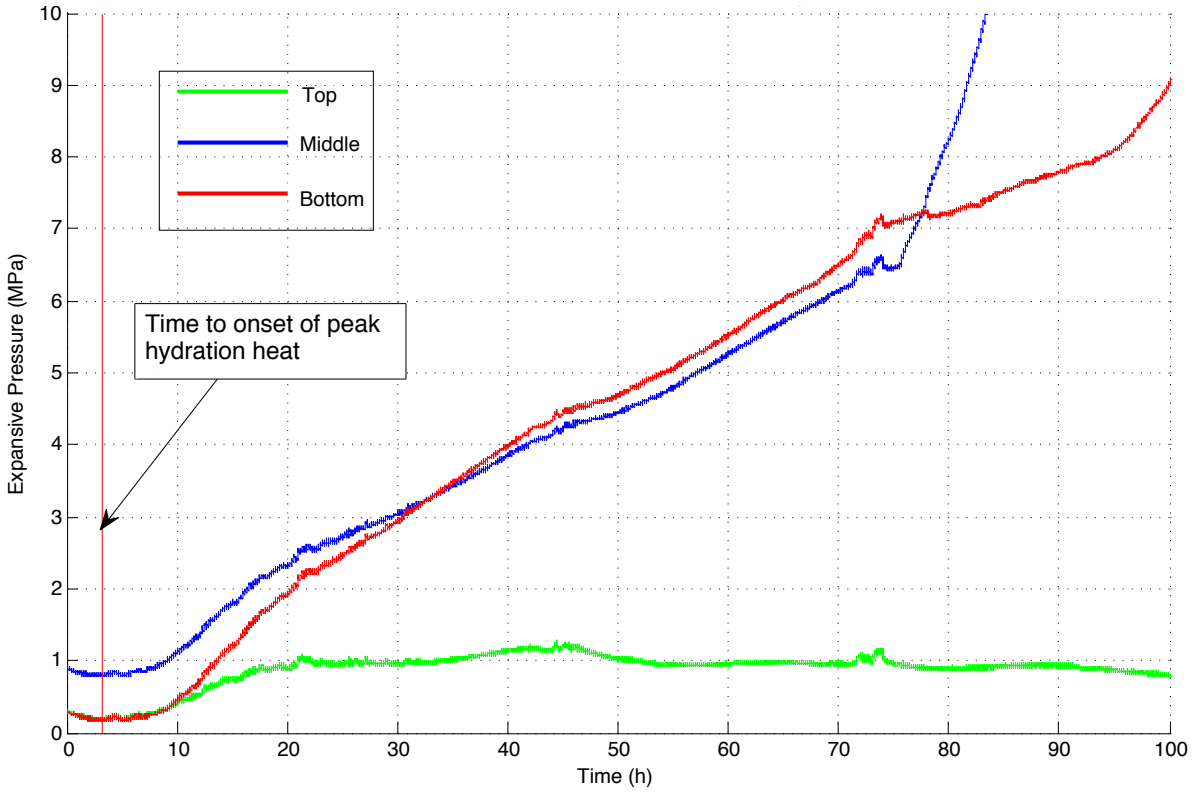

Figure 9. Expansive pressure development over 100 hours in the 101.6 mm pipe in detail

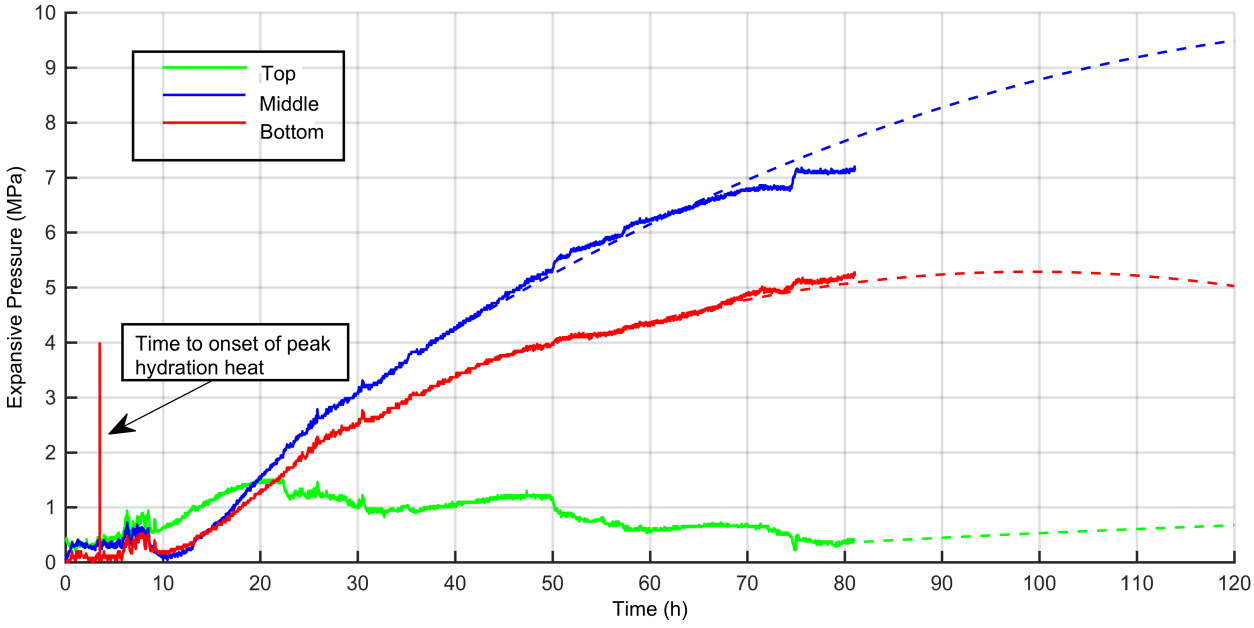

Figure 10. Expansive pressure development over 120 hours in the 76.2 mm pipe (Dotted line is a projection)

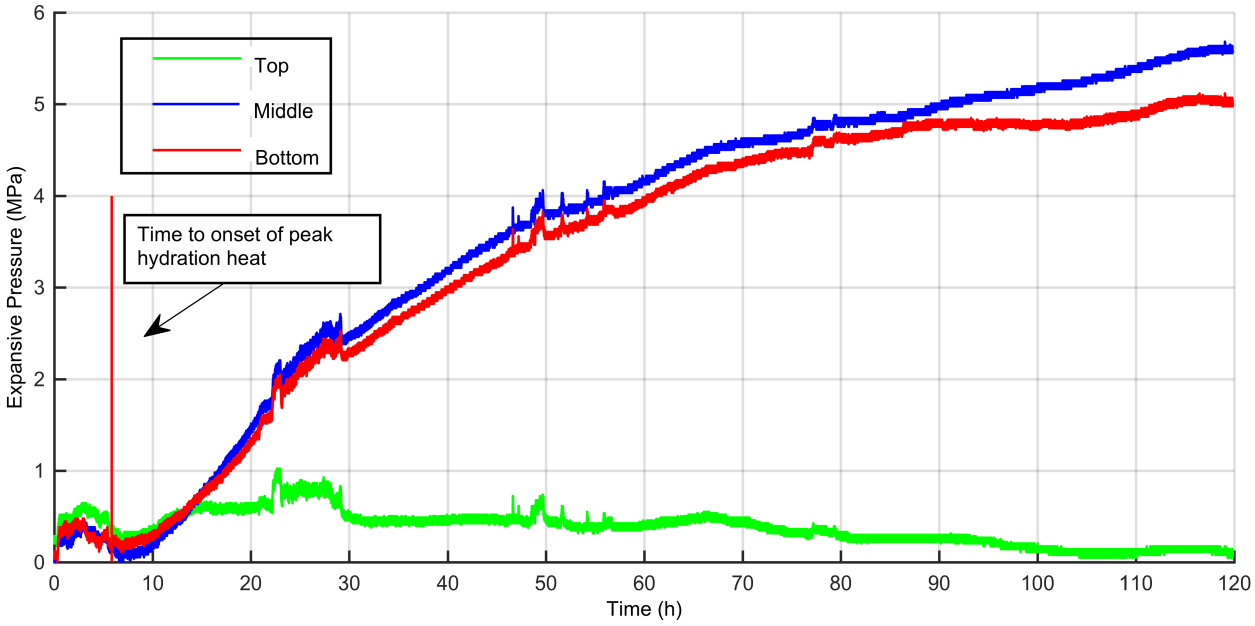

Figure 11. Expansive pressure development over 120 hours in the 50.8 mm pipe

Experimental results presented herein generally showed that bigger diameter specimens resulted in larger expansive pressures (Figs. 8-11). However, the expansive pressure development rate was not linear with borehole diameter. Thus, halving the diameter from 101.6 mm to 50.8 mm (quartering the volume) lead to a 680% reduction in expansive pressure development. Whereas a 50% decrease in diameter from the 76.2 mm pipe to the 50.8 mm pipe (half the other volume change) only generated a 200% reduction in pressure. Thus, explaining changes of behaviour by volume (as opposed to diameter, as has been previously done) is more useful. Halving pipe volume (2280.13 cm^3 vs. 1013.41 cm^3) halved the pressure, while decreasing the pipe volume by approximately 75% (4053.66 cm^3 vs. 1013.41 cm^3) decreased the expansive pressure development by approximately 85% (38 MPa vs. 5.5 Mpa). These results show that changing the size of the pipe changes the expansive pressure but not in a wholly linear manner. The exact impacts of diameter and volume also remain unknown.

343 Pipe size also changed the pressure generation cycle. Specifically, peak expansive
344 pressure only started to develop at the onset of peak hydration heat. For example, at just over 120
345 hours, maximum expansion pressure reached 38 MPa at mid-height of the 101.6 mm diameter
346 pipe, in contrast to the predicted expansive pressures of 9.8 MPa for the 76.2 mm pipe and
347 almost 5.56 MPa in the middle of 50.8 mm diameter pipe.

348 These results also showed that the SCDA in the larger diameter pipes resulted in more
349 rapid pressure gains. In the largest pipe, the expansive pressure at the middle of the pipe started
350 to develop after 5.9 hours compared to 6.2 hours for the 76.2 mm pipe, and 8.5 hours for the
351 smallest pipe. Expansive pressures at 24 hours at the middle of the pipes were 2.7 MPa
352 (101.6 mm), 2.3 MPa (76.2 mm) and 2.1 MPa (50.8 mm). In summary, larger diameter pipes
353 (and their larger volumes of SCDA) resulted in earlier and greater hydration heat levels, which
354 resulted in faster chemical reactions and greater expansive pressures.

355 Expansive pressure development was also impacted by the volume of material, with
356 variation within the specimen. It was fastest in the largest pipe at 75 hours for the middle of the
357 sample and 103 hours at the bottom; the same trend was recorded by Natanzi et al. [9]. After 80
358 hours, expansive pressure at the middle of the biggest pipe was double that of the smallest pipe.
359 Therefore, increasing pipe volume by almost 400% (1013.41 cm^3 vs. 40553.66 cm^3) nearly
360 doubled the expansive pressure development (4.6 MPa vs. 8.3 MPa) in the water bath samples
361 within the 4-day experimental window.

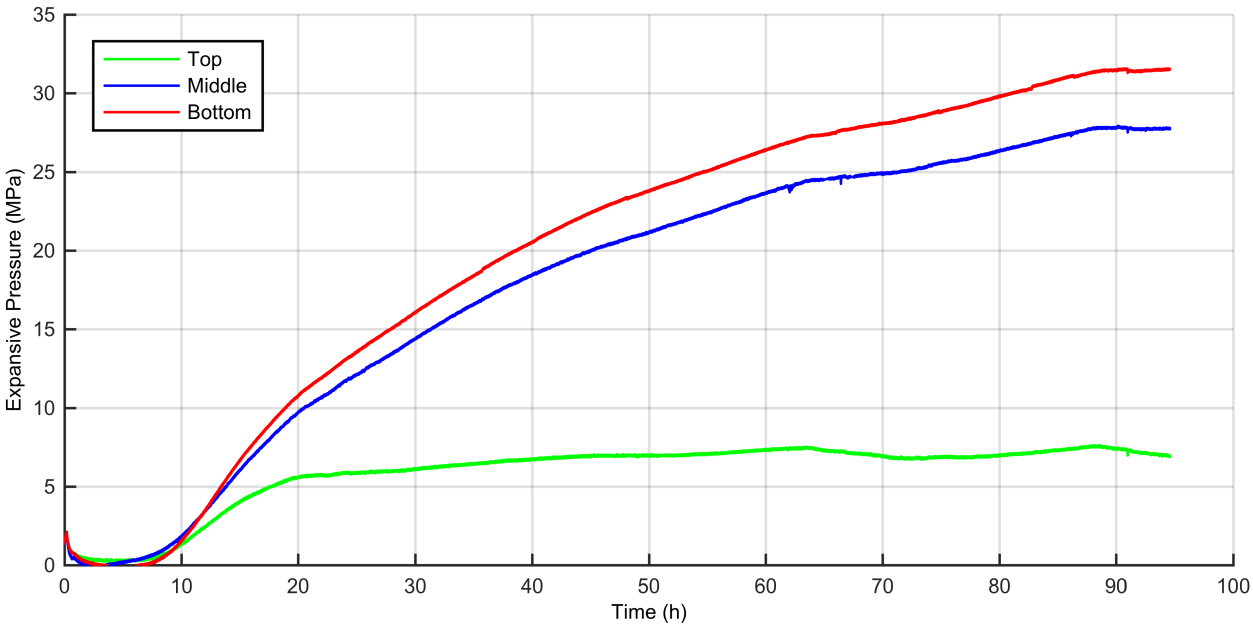

Figure 12. Expansive pressure development over 4 days in 50.8 mm pipe at temperature - controlled chamber at 10°C

When compared to the expansive pressure generated in the chamber (Figure 12), the water bath samples had smaller pressures that developed later, thus following the above-reported temperature trends (Figure 11). The other difference was the high expansive pressure at the bottom of the pipe in the chamber (32 MPa) versus that which developed in the water bath (only 5.1 MPa). Overall, the chamber specimen was warmer, as the space was relatively confined and had a slower compensation mechanism to dissipate the hydration heat development. Overall, the warmer chamber specimen generated over 6 times more expansive pressure than the cooler water bath specimen of the same diameter.

4.3 Vertical Expansion

During testing, the SCDA expanded upward beyond the geometry of the testing cylinder (see Figure 13). This vertical expansion was measured at the end of testing (five days from the start of

testing). Vertical expansions of 149.6 mm, 72.73 mm, and 60.68 mm were measured for the 101.6 mm, 76.2 mm, and 50.8 mm pipes, respectively. The bigger borehole diameter clearly resulted in the greater vertical expansion. Considering a linear coefficient of stainless steel α=0.000012/°C and the relatively small temperature changes, the radial expansion was negligible. Results showed that reducing the diameter from 101.6 mm to 50.8 mm caused an almost 20% decrease in the vertical expansion.

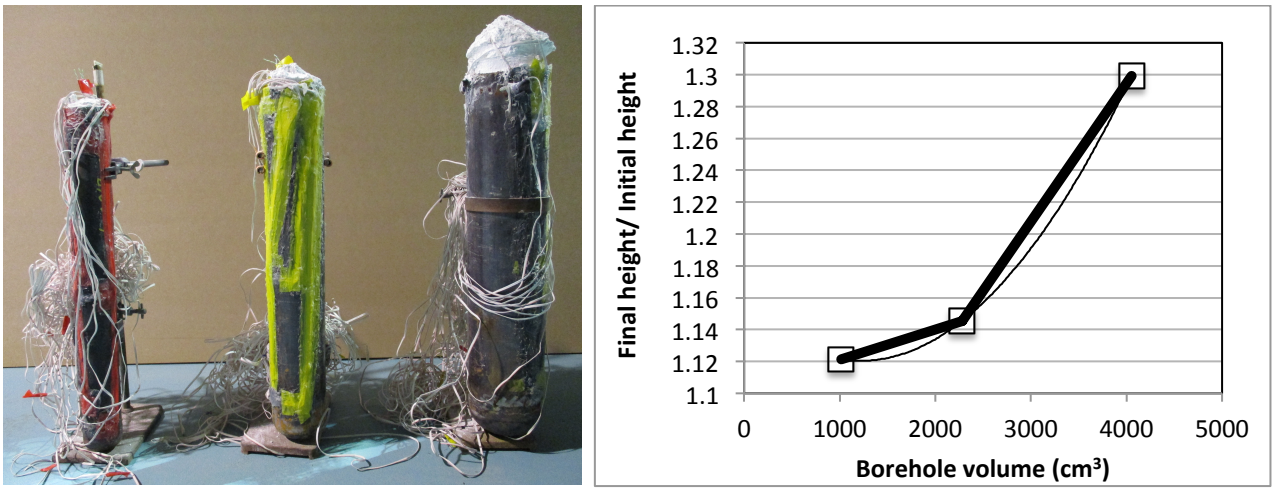

(a) Photograph of the pipes after testing. (b) Ratio of height change by borehole volume.

Figure 13. SCDA vertical expansion.

5 DISCUSSION

Figure 14 provides a summary graph. When considering the area of the pipe there are fairly linear correlations between the size and three main outputs: (1) peak hydration heat temperature; (2) inverse of the time to onset of the peak hydration heat; and (3) volumetric expansion. The onset of the hydration heat has been shown to correlate with the initiation of the pressure development and with higher and earlier expansion pressures. Within the time frame of the testing (which was selected with a construction schedule in mind), the peak pressure was not

captured, but as demonstrated in the previous section, halving the pipe area halved the pressure at the end of testing. As the main reaction (which generates heat of hydration and in return expansive pressure) is exothermic, ambient temperature plays a significant role as previously demonstrated [9]. Specifically, higher ambient temperature accelerates the exothermic reaction and generates more pressure and heat.

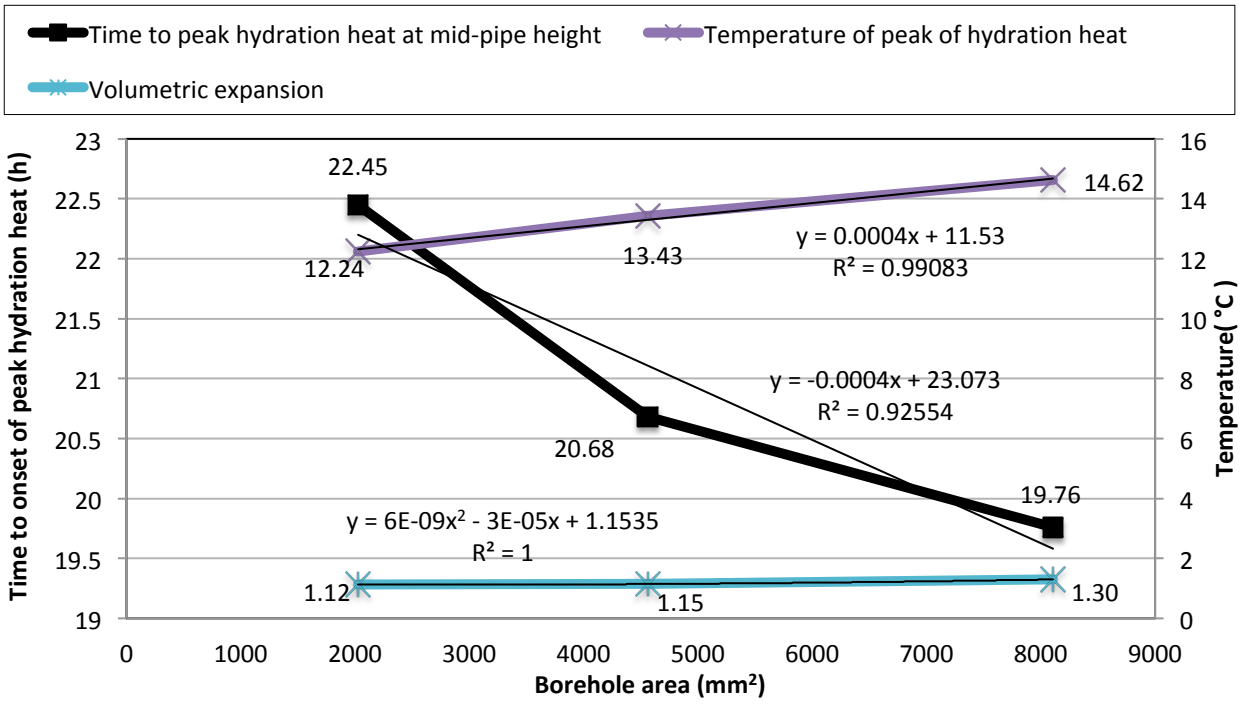

Figure 14. Linear correlations between the size and peak hydration heat temperature; time to onset of peak hydration heat; and volumetric expansion ratio

5.1 Heat of hydration

The wider pipes generated a faster onset of hydration heat and higher peaks (Figs. 2-4). Similar results were shown experimentally by Ishida et al. [19] in 300 mm cubes of mortar with the

SCDA centered in 50 mm diameter holes, 260 mm in depth (Figure 15) and by Natanzi et al. [9] in 170 mm long pipes, 36 mm in diameter.

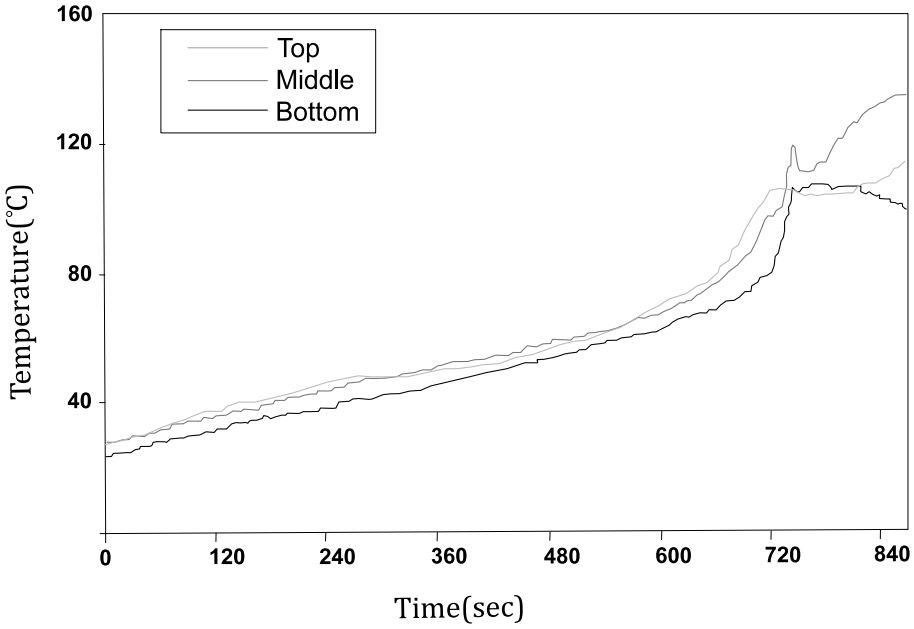

Figure 15. Heat of hydration generation and progress in a 50 mm pipe [19].

The research undertaken herein showed that at 10°C in the chamber conditions in a 50.8 mm diameter pipe, the peak of hydration heat occurred after only 10.79 hours at 17.79°C versus the required 22.45 hours at 12.10°C for the specimen in the water bath. These findings reflect previous research. For example, in experimental work by Harada et al. [25] in a 33 mm steel pipe in a 20°C water bath, the peak hydration heat was 1-2°C higher than the surrounding water, but the difference grew to 23°C when the pipe was surrounded by 30°C air (Figure 16). Those results and the ones demonstrated herein illustrate the importance of the thermal transfer issue and the need to further model this, if a robust expansion pressure prediction tool is to be created. Another factor that must also be considered is the double peak in the smallest diameter pipe. This was also previously reported by Harada et al. [25] in the above referenced experiment.

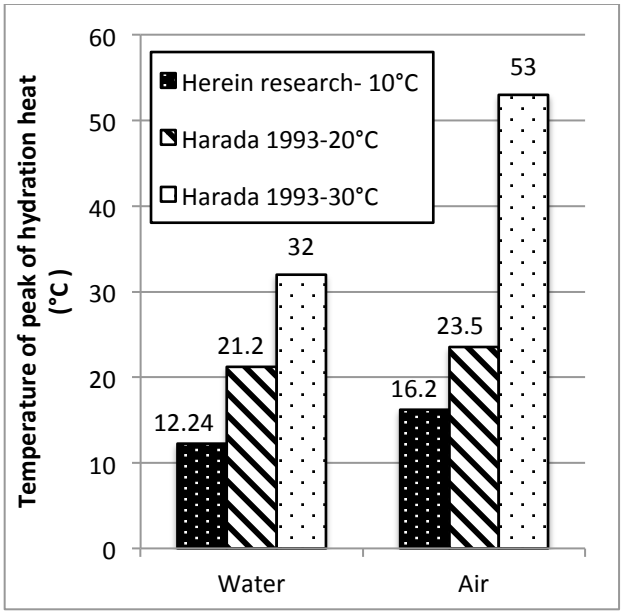

419

420 **Figure 16.** Influence of surrounding material on peak of hydration heat in (some data from

421 Harada et al. [25])

422 **5.2 Expansive pressure**

423 The pipe size significantly affected the rate and magnitude of expansive pressure development
424 with larger and more accelerated results in larger specimens. Importantly, an increase in the pipe
425 diameter is also an enlargement of its volume and that of the SCDA contained, which influenced
426 the heat of hydration, $Ca(OH)_2$ generation, and expansive pressure development directly. In a
427 20°C water bath experiment by Soeda et al. [26] with an SCDA mixed with 30% water, in a
428 300 mm long steel pipe, increasing the pipe volume from 212.06 cm^3 to 589.05 cm^3 (diameter
429 from 30 mm to 50 mm) increased the maximum recorded expansive pressure by almost 30%.
430 Those findings and the ones reported herein appear to contradict the earlier work by Dowding
431 and Labuz [17] who saw no discernible difference in the first 48 hours in thick-walled steel
432 cylinders with a volume change of 4519.18 cm^3. While their initially reported behavior was
433 similar to that shown in the study herein at a much colder temperature (10°C vs. 22°C), the later

behaviours differed greatly – up to 5 MPa at 48 hours. In contrast, research by Hinze and Brown [7], reported that volume change was not a significant variable in expansive pressure development in the first 24 hours with a change of SCDA volume of only 441.79 cm^3.

Expansive pressure was significantly influenced by heat of hydration temperature, which was definitively impacted by the pipe volume (see Figure 17). After 80 hours, while expansive pressure remained less than 10 MPa in all pipes, pressure in the largest pipe was double that in the smallest pipe. After 120 hours, this difference in expansive pressure grew to almost 7 times.

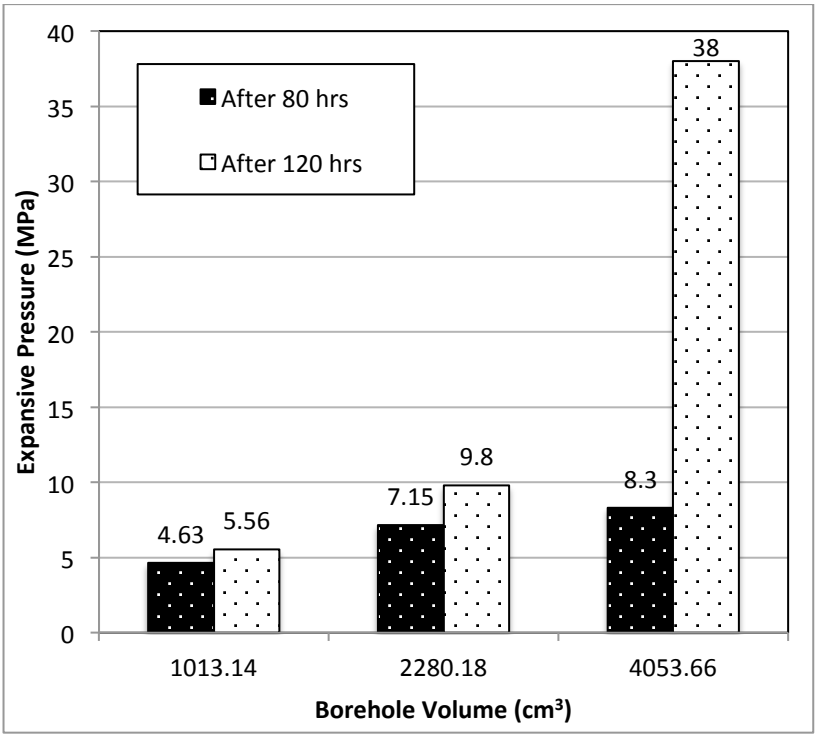

Figure 17. Mid-height expansive pressure development different pipe volumes

5.3 Volumetric Expansion

Borehole diameter also had a notable effect on SCDA's volumetric expansion, which was caused by the exothermic reaction between CaO and water [25]. In the research undertaken herein, in

447 the largest diameter pipe, the volumetric expansion of SCDA was almost 1.3 times, while in the
448 smallest only 1.12 times. Similarly, at the same ambient temperature of 10°C, Natanzi et al. [9]
449 recorded a 1.3 times increase when measuring the expansion of Bristar in a 170 mm high, 36 mm
450 diameter steel pipe placed in a temperature-controlled chamber environment.

451 While a theoretical expansion value was calculated as 1.95 based on the molar
452 weights and the specific gravity of CaO and $Ca(OH)_2$, this was confirmed by Fukui ([27],
453 who reported 1.96 based on microscope observations of the degree of expansion from CaO
454 to $Ca(OH)_2$. This was further affirmed by Chatterji [28], who reported molar solid volume
455 expansion of about 90% during CaO hydration. There are multiple theories and models
456 explaining ettringite formation and expansion, but they can be divided into two main
457 groups: (1) crystal growth theory and (2) swelling theory. Crystal growth theory
458 hypothesizes that expansion is caused by increasing ettringite crystals, which form on the
459 surfaces of the SCDA particles or in the resulting solution. This crystal growth causes a
460 crystallisation pressure followed by expansive pressure gain. In contrast, swelling theory
461 hypothesizes that expansion is caused by a combination of water-adsorption and the
462 swelling characteristics of the ettringite gel, which forms by means of a through-solution
463 mechanism due to the reaction between the expansive particles and the surrounding
464 solution. The presence of calcium hydroxide ($Ca(OH)_2$) in solution results in the formation
465 of colloidal-sized ettringite particles and the absence of calcium hydroxide ($Ca(OH)_2$)
466 results in the creation of larger ettringite particles [29]. Further insight is likely only to be
467 gained through CT-scanning.

468 SCDAs are very thermally sensitive, therefore the temperature of the confining material
469 needs careful consideration. If the temperature of the surrounding, confining materials is very

low, the heat of hydration and expansive pressure can be heavily impacted. Other considerations such as changing borehole geometry and spacing could be considered if there is a limitation on cracking time. Finally, a slight difference in ambient temperature can cause significant changes in SCDA behaviour as reported by Natanzi et al. [9], where increasing the ambient temperature from 19°C to 21°C in a chamber test caused an SCDA blow out.

6 CONCLUSIONS & RESEARCH SIGNIFICANCE

This paper investigated the impact of borehole diameter, volume and thermal transfer in a commercial SCDA (Bristar) tested at 10℃. The relationships between the heat of hydration, expansive pressure, thermal transfer, and volumetric expansion were investigated in a section of steel pipe of various diameters. The heat of hydration was recorded by embedded thermocouples at five locations in and around the pipe and paired with strain gauges where possible.

Experimental results showed that the largest diameter pipe had a peak hydration heat temperature almost 50% greater than the surrounding 10°C water versus only about 22% for the smallest pipe (14.62°C vs. 12.24°C). Specifically, quadrupling the pipe volume (doubling the pipe diameter) accelerated the time to onset of peak hydration heat generation by almost 177%. The larger pipe contained more SCDA and thus more CaO, which resulted in an accelerated onset of peak hydration heat (14%). This resulted in faster and larger expansive pressure development. Quadrupling the pipe volume from 1013.14 cm^3 to 4053.66 cm^3 caused a 680% increase in expansive pressure development after 120 hours, whereas the 50% volume increase only doubled the pressure in the same time period. Quadrupling the pipe volume from 1013.14 cm^3 to 4053.66 cm^3 also caused an almost 20% increase in volumetric expansion at the top of the pipe.

493 An equivalent small diameter sample in a constant temperature chamber (as opposed to
494 the large heat sink of a large water bath) showed a 5°C higher hydration heat, which resulted in a
495 six-fold difference in expansive pressure after 4 days of testing and an order of magnitude more
496 pressure in the first day (the critical time period of construction usage). These tests provide
497 critical insights into the previously recorded performance discrepancies for the onset of cracking
498 in large concrete blocks and in situ field conditions compared to that reported by SCDA
499 manufacturers. The results also imply that the results of many previously reported tests
500 conducted in pipes cannot be directly used to predict SCDA field performance, as they fail to
501 account for the negative influence of thermal transfer.
502
503 **ACKNOWLEDGMENTS**
504 The authors would like to thank Mr. Derek Holmes and Mr. John Ryan, lab technicians at the
505 University College Dublin for their tireless efforts in the lab throughout the research and summer
506 intern Ms. Renata Wercelens for assistance with data collection.
507
508 **FUNDING**
509 This work was funded by Science Foundation Ireland [grant 12/ERC/12534]; and Enterprise
510 Ireland [grant IP20150410Y].
511
512 **REFERENCES**
513 [1] Mather B. Expansive cement. Vicksburg (MI): United States Army Engineer Waterways
514 Experiment Station; 1970. Report No.: AD-A030 953.

515 [2] Hayashi H, Soeda K, Hida T, Kanbayashi M. Non-explosive demolition agent in Japan. In:
516 Lauritzen EK, editor. Demolition and Reuse of Concrete and Masonry. Proceedings of the
517 Third International RILEM Symposium, London: Chapman & Hall; 1993, p. 231-41.
518 [3] Wang YS, You BK and Zhang GQ. Application of soundless cracking agent in China. In:
519 Kasai Y, editor. Demolition and Reuse of Concrete and Masonry 2nd International RILEM
520 Symposium, 1988 Nov 7-11; Tokyo. London: Chapman & Hall; 1988, p. 149-57.
521 [4] Laefer DF, Ambrozevitch-Cooper N, Huynh MP, Midgette J, Ceribasi S, Wortman J.
522 Expansive fracture agent behaviour for concrete cracking. Mag Concr Res 2010;62(6):443-
523 452. DOI:10.1680/macr.2010.62.6.443.
524 [5] Huynh, M.P., Laefer, D.F., McGuill, J. and White, A., 2017. Temperature-related
525 performance factors for chemical demolition agents. International Journal of Masonry
526 Research and Innovation, 2(2-3), pp.220-240.
527 [6] Gambatese JA. Controlled concrete demolition using expansive cracking agents. J Constr
528 Eng Manag ASCE 2003;129(1):98-104. DOI: 10.1061//(ASCE)0733-9364(2003)129:1/98.
529 [7] Hinze J, Brown J. Properties of soundless chemical demolition agents. J Constr Eng Manag
530 ASCE 1994;120(4):816-827.
531 [8] Goto K, Kojima K, Watabe K. The mechanism of expansive pressure and blow-out of static
532 demolition agent. In: Kasai Y, editor. Demolition and Reuse of Concrete and Masonry 2nd
533 International RILEM Symposium, 1988 Nov 7-11; Tokyo. London: Chapman & Hall; 1988,
534 p. 132-40.
535 [9] Natanzi AS, Laefer DF, Connolly L. Cold and moderate ambient temperatures effects on
536 expansive pressure development in soundless chemical demolition agents. Constr Build
537 Mater 2016;110:117-27. DOI: 10.1016/j.conbuildmat.2016.02.016.

538 [10] Étkin MB, Azarkovich AE. Effect of non-explosive splitting compounds and rational work
539 parameters. Power Technol Eng 2006;40(5):287-92.
540 [11] Connolly, L. Ambient temperature, expansive pressure and heat of hydration in soundless
541 chemical demolition agent [thesis]. Dublin, Ireland: University College Dublin; 2013.
542 [12] Onoda Cement Company. Bristar—Nonexplosive Demolition Agent. Tokyo: Onoda
543 Cement Company; 1980.
544 [13] Polivka M. Factors influencing expansion of expansive cement concretes. ACI Special Publ
545 1973;38:239-250. DOI: 10.14359/17206
546 [14] Soeda K, Harada T. The mechanics of expansive pressure generation with expansive
547 demolition agent. Trans JSCE 1993;19:121-35.
548 [15] Bristar (2016) BASF Construction Chemicals UK Ltd, Manchester, United Kingdom
549 http://www.epms-supplies.co.uk/admin/products/documents/BASF%20(Feb%20-
550 %20MBT)/Health/POWERBRISTARMSDS.pdf [Accessed 28 June 2018].
551 [16] Soeda K, Tsuchiya K, Matsuhisa M, Harada T. The properties of the expansive stress of
552 non-explosive demolition agent in long period of time. Gypsum & Lime 1994;248:37-43.
553 [17] Dowding CH, Labuz JF. Fracturing of rock with expansive cement. J Geotech Eng ASCE
554 1982;109:1288-99.
555 [18] Schram CM, Hinze J. Fracturing of rock using expansive soundless chemical demolition
556 agents. In: Kulhawy FH, editor. Foundation Engineering: Current Principles and Practices,
557 New York: ASCE; 1989, p. 447-58.
558 [19] Ishida T, Suemune K, Fukui H and Kinoshita N. Effect of thermal stress in fracturing by
559 expansive cement agent in comparison with a borehole pressurizing test and a heater test.
560 In: Alaska Rocks 2005. Proceedings of the 40th US Rock Mechanics Symposium, 2005 Jun

561 25-29; Anchorage, AK. Alexandria (VA): American Rock Mechanics Association; 2005,
562 vol. 3, p. 940-8.
563 [20] Timoshenko SP and Goodier JN. Theory of elasticity. New York: McGraw Book
564 Company; 1951.
565 [21] Hertzberg, RW. Deformation and Fracture Mechanics of Engineering Materials. 4th ed.
566 Hoboken (NJ): John Wiley & Sons Inc.; 1996.
567 [22] Huynh M-P, Laefer DF. Expansive cements and soundless chemical demolition agents:
568 state of technology review. Paper presented at: 11th Conference on Science and
569 Technology; 2009 Oct 21-23; Ho Chi Minh City.
570 [23] Natanzi AS, Laefer DF. Using chemicals as demolition agents near historic structures. In:
571 Meli R, Peña F, Chavez M, editors. Proceedings of 9th International Conference on
572 Structural Analysis of Historical Constructions, 2014 Oct 14-17; Mexico City. [place
573 unknown: publisher unknown]; 2014, Paper 128.
574 [24] Natanzi, A. S. (2017). Soundless chemical demolition agents performance under cold
575 and cool temperatures in concrete and masonry structures. Doctoral Thesis,
576 University College Dublin, Ireland.
577 [25] Harada T, Soeda K, Idemistzu T, Watanabe A. Characteristics of expansive pressure of an
578 expansive demolition agent and the development of new pressure transducers. Trans Jpn
579 Soc Civ Eng 1993;1993(478):95-109.
580 [26] Soeda K, Yamada S, Nakashima Y, Nakaya S, Haneda H, Izawa N. Non-explosive
581 demolition agent. In: Kasai Y, editor. Demolition and Reuse of Concrete and Masonry 2nd
582 International RILEM Symposium, 1988 Nov 7-11; Tokyo. London: Chapman & Hall;
583 1988, p. 116-125.

584 [27] Fukui H. Static demolition by calcium oxide. J Jpn Explos Soc 1996;57(2):62-70.
585 [28] Chatterji S. Mechanism of expansion of concrete due to the presence of dead-burnt CaO
586 and MgO. Cement and Concrete Research. 1995 Jan 1;25(1):51-6.
587 [29] Cohen MD. Theories of expansion in sulfoaluminate-type expansive cements: schools of
588 thought. Cement and Concrete Research. 1983 Nov 1;13(6):809-18.